

Thermal diffusivity and conductivity of supercooled liquid in $Zr_{41}Ti_{14}Cu_{12}Ni_{10}Be_{23}$ metallic glass

Michiaki Yamasaki,^{a)} Shinya Kagao, and Yoshihito Kawamura

Department of Materials Science, Kumamoto University, Kurokami, Kumamoto 860-8555, Japan

Kenji Yoshimura

Mechanics and Electronics Research Institute, Fukuoka Industrial Technology Center, Yahatanishi-ku, Kitakyusyu 807-0831, Japan

(Received 30 September 2003; accepted 13 April 2004; published online 19 May 2004)

We measured the thermal diffusivity of amorphous solid and supercooled liquid in a $Zr_{41}Ti_{14}Cu_{12}Ni_{10}Be_{23}$ bulk metallic glass (BMG) and its crystalline counterpart alloy at temperatures ranging from room temperature to 700 K, using a laser flash method. The thermal diffusivity and conductivity of the amorphous solid were weakly temperature dependent and increased with increasing temperature up to the glass transition temperature. The thermal diffusivity of the supercooled liquid was approximately $3.5 \times 10^{-6} \text{ m}^2 \text{ s}^{-1}$ and quite constant with temperature. The amorphous solid and supercooled liquid of $Zr_{41}Ti_{14}Cu_{12}Ni_{10}Be_{23}$ BMG showed lower thermal diffusivity and conductivity than the crystalline counterpart in the range from room temperature to crystallization temperature. © 2004 American Institute of Physics. [DOI: 10.1063/1.1759768]

New families of bulk metallic glasses (BMGs) with high glass-forming ability¹ have been discovered, such as Pd-Cu-Ni-P,² La-Al-Ni-Cu-Co,³ Mg-Cu-Y,⁴ Cu-Zr-Ti,⁵ Ti-Zr-Cu-Ni,⁶ Zr-Ni-Al-Cu⁷ and Zr-Ti-Cu-Ni-Be.⁸ The BMGs are characterized by the high thermal stability of their supercooled liquid, which permits study of the thermophysical properties of the supercooled liquid in addition to the amorphous metallic solid. The thermophysical properties of metallic supercooled liquid rouse our interest not only for fundamental studies but also for studies of potential practical applications. In fundamental studies, the thermophysical properties are required to clarify the glass formation mechanism and to estimate the critical cooling rate for formation of amorphous single phase and the critical heating rate⁹ for heating amorphous alloys without devitrification. Recent application studies of BMGs include many attempts to make connections to BMGs.^{10–12} Many successful welding methods can make connections to BMGs, including friction,^{13–15} pulse current,¹⁶ explosion,¹⁰ laser-beam, and electron-beam welding.^{17–19} Pulse current, explosion, laser-beam, and electron-beam weldings are liquid phase methods. To determine the optimum conditions for welding BMGs without crystallization with the several liquid phase methods, it is necessary to investigate the thermal history during welding. In order to clarify the thermal history, the thermal properties such as specific heat capacity, thermal diffusivity and thermal conductivity are required. Previous reports have supplied thermodynamic and kinetic data for BMGs, including specific heat capacity,^{20–23} viscosity^{24–26} and heats of transformation of their amorphous solid.^{27,28} However, there has been no report of the thermal diffusivity and thermal conductivity of their supercooled liquid. The aim of this study is to clarify the thermal conductivity and diffusivity of amorphous solid and supercooled liquid in a

typical $Zr_{41}Ti_{14}Cu_{12}Ni_{10}Be_{23}$ (at. %) BMG and its polycrystalline counterpart alloy. This letter presents the first measurement of thermal conductivity of the supercooled liquid in BMGs.

A master alloy ingot with the nominal composition $Zr_{41}Ti_{14}Cu_{12}Ni_{10}Be_{23}$ (at. %) was prepared by arc melting a mixture of pure zirconium, titanium, copper, nickel and beryllium in a Ti-gettered argon atmosphere. $Zr_{41}Ti_{14}Cu_{12}Ni_{10}Be_{23}$ BMG sheet was prepared from master alloy by rapid-quench copper mold casting method in which the cooling rate reaches more than 100 K/s. BMG disks with a thickness of 1.2 mm and a diameter of 10 mm were trimmed off the cast BMG sheet. The glass transition temperature, T_g , crystallization temperature, T_x , and critical cooling rate, R_c , of the $Zr_{41}Ti_{14}Cu_{12}Ni_{10}Be_{23}$ BMG are 623 K, 672 K, and 1 K/s, respectively.²⁹

The thermal diffusivity of BMG has been measured between 300 and 700 K with a ULVAC-RIKO TC-7000 Standard Laser Flash Thermal Constants Analyzer. Prior to the measurement, the surface of the BMG disks was blackened by immersion in the 0.5% aqueous HF solution for 0.5 min in order to improve the absorption of the laser beam. The sample was clamped on an alumina sample holder. The whole assembly was enclosed in a chamber evacuated to below 10^{-2} Pa. The temperature was raised from room temperature to each test temperature with a heating rate of 20 K/min and then kept at each temperature for more than 10 min. Thereafter, the thermal diffusivity measurement was carried out under isothermal conditions. A laser pulse with a wavelength of 694 nm and a diameter of 10 mm was provided by a normal oscillation-type ruby laser with a frequency multiplier. The maximum temperature of the rear surface of the sample was measured by thermocouple and infrared temperature sensor.

Thermal diffusivity was calculated by the “ $t_{1/2}$ method”.³⁰ The temperature of the rear surface of the speci-

^{a)}Author to whom correspondence should be addressed; electronic mail: yamasaki@gpo.kumamoto-u.ac.jp

men changes according to the following equation³¹

$$T(t) = T_M \left[1 + 2 \sum_{n=1}^{\infty} (-1)^n \exp\left(-n^2 \frac{t}{t_0}\right) \right], \quad (1)$$

where $T_M = Q/\rho C_p \ell$, the maximum temperature rise of the rear surface of the specimen with no heat loss; Q is the pulse of radiant energy in J cm^{-2} ; C_p , the heat capacity of the specimen, and $t_0 = \ell^2/(\pi^2 \alpha)$, the characteristic time of thermal diffusion; ℓ , the thickness of the specimen, and α , the thermal diffusivity in $\text{cm}^2 \text{s}^{-1}$.

Two dimensionless parameters, V and ω , can be defined

$$V(t) = T(t)/T_M \quad (2)$$

$$\omega = \pi^2 \alpha t / \ell^2. \quad (3)$$

T_M denotes the maximum temperature at the rear surface. The combination of Eqs. (1), (2) and (3) yields

$$V = 1 + 2 \sum_{n=1}^{\infty} (-1)^n \exp(-n^2 \omega). \quad (4)$$

When V is 0.5 and ω is 1.37, thermal diffusivity, α , is represented by the following equation:

$$\alpha = 1.37 \frac{\ell^2}{\pi^2 t_{1/2}}. \quad (5)$$

The half rise time, $t_{1/2}$, is defined by the interval required for the rear surface temperature to reach one half of the maximum temperature.

The thermal conductivity κ was calculated from the diffusivity, α , from the relation

$$\kappa = \rho C_p \alpha. \quad (6)$$

The specific heat, C_p , of samples was given by

$$C_p = \frac{Q}{\rho \ell T_M}. \quad (7)$$

The pulse of radiant energy, Q , was calculated from the known specific heat of sapphire plate and the T_M measured for sapphire.

Figure 1 shows the change in the thermal diffusivity, α , of $\text{Zr}_{41}\text{Ti}_{14}\text{Cu}_{12}\text{Ni}_{10}\text{Be}_{23}$ BMG and its crystalline alloy as a function of temperature. The thermal diffusivity of the amorphous solid was weakly dependent on temperature and increased with increasing temperature up to the glass transition temperature. The thermal diffusivity of the supercooled liquid was approximately $3.5 \times 10^{-6} \text{ m}^2 \text{ s}^{-1}$ and quite constant with temperature. The $\text{Zr}_{41}\text{Ti}_{14}\text{Cu}_{12}\text{Ni}_{10}\text{Be}_{23}$ BMG showed a lower thermal diffusivity than its crystalline counterpart in the range from room temperature to crystallization temperature. These phenomena were explained by the obvious fact that the BMGs are considered to be highly alloyed solid solutions and their densities are smaller than their crystalline counterparts. Crystallization causes an increase in thermal diffusivity to $5.5 \times 10^{-6} \text{ m}^2 \text{ s}^{-1}$. The amorphous solid is characterized by small positive temperature coefficients of diffusivity, as is its crystalline counterpart.

Figure 2(a) shows the change in the thermal conductivity, κ , for $\text{Zr}_{41}\text{Ti}_{14}\text{Cu}_{12}\text{Ni}_{10}\text{Be}_{23}$ BMG and crystalline alloy as a function of temperature. In the amorphous solid state, the

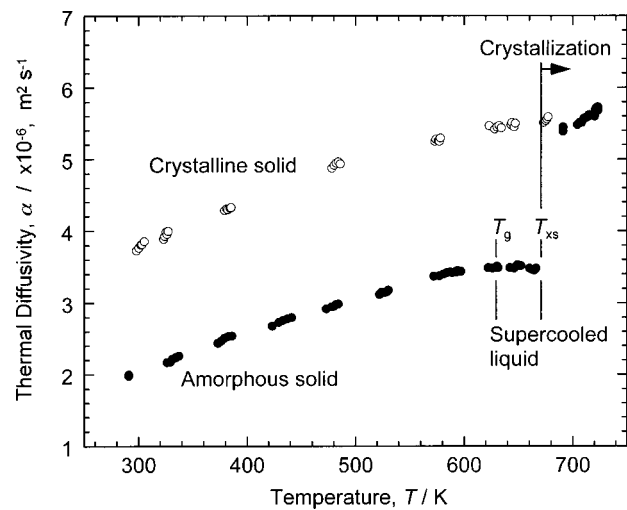


FIG. 1. Change in the thermal diffusivities of $\text{Zr}_{41}\text{Ti}_{14}\text{Cu}_{12}\text{Ni}_{10}\text{Be}_{23}$ BMG (solid circles) and crystalline alloy (open circles) as a function of temperature. T_g and T_{xs} denote glass-transition temperature and onset of crystallization temperature, respectively.

thermal conductivity, as well as the thermal diffusivity, were weakly temperature dependent, with small positive temperature coefficients. The thermal conductivity rose dramatically to $15 \text{ W m}^{-1} \text{ K}^{-1}$ at the glass transition temperature, T_g . In the supercooled liquid state, the thermal conductivity de-

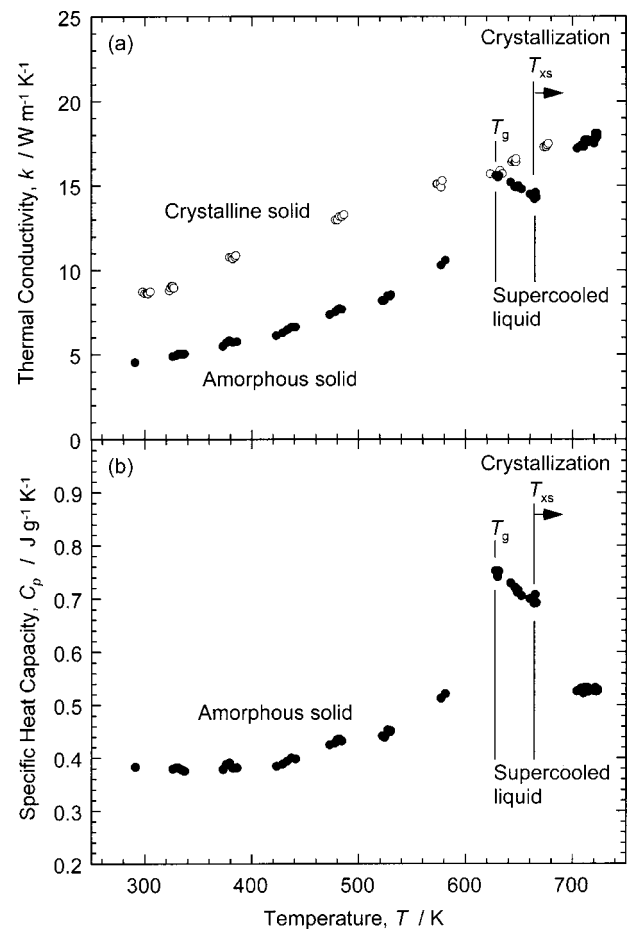


FIG. 2. Change in the thermal conductivity (a) and specific heat (b) of $\text{Zr}_{41}\text{Ti}_{14}\text{Cu}_{12}\text{Ni}_{10}\text{Be}_{23}$ BMG (solid circles) and crystalline alloy (open circles) as a function of temperature. T_g and T_{xs} denote glass-transition temperature and onset of crystallization temperature, respectively.

TABLE I. Electrical conductivity and thermal conductivity of Zr- and Pd-based metallic glasses (rows 3–5, cited from Ref. 27)

Metallic glass	Electric conductivity ($\mu\Omega\text{m}$) ⁻¹	Thermal conductivity, κ ($\text{Wm}^{-1}\text{K}^{-1}$), at 300 K			
		Total, κ	Electronic, κ_{electron}	Phonon, κ_{phonon}	$\kappa_{\text{phonon}}/\kappa$
Zr ₄₁ Ti ₁₄ Cu ₁₂ Ni ₁₀ Be ₂₃	0.438	4.59	3.22	1.37	0.30
Pd ₄₀ Ni ₄₀ P ₂₀	0.826	7.03	6.07	0.96	0.14
Pd ₄₀ Ni ₂₀ Cu ₂₀ P ₂₀	0.699	6.25	5.14	1.11	0.18
Pd ₄₀ Ni ₁₀ Cu ₃₀ P ₂₀	0.541	5.11	3.97	1.13	0.22

clined slightly with increasing temperature. Crystallization brought about an increase in thermal conductivity. It is natural that the thermal conductivity of fully crystallized BMG was in a good agreement with that of the crystalline counterpart alloy.

As shown in Fig. 2(b), The specific heat of the Zr₄₁Ti₁₄Cu₁₂Ni₁₀Be₂₃ BMG showed discontinuous changes with temperature at its glass-transition and crystallization temperatures. The specific heat of the supercooled state was higher than that of the amorphous solid.

The product of specific heat and density, $C_p\rho$, the thermal diffusivity, α , and thermal conductivity, κ , may be thought of as a material's ability to store heat, to transmit temperature and to transfer heat, respectively. The thermal diffusivity, α , is inversely proportion to the heat storage ability, $C_p\rho$, and is proportional to the thermal conductivity, κ , as shown in Eq. (6). The supercooled liquid in the Zr₄₁Ti₁₄Cu₁₂Ni₁₀Be₂₃ BMG had higher heat-transfer and heat-storage abilities than its amorphous solid. In the supercooled liquid region, the gain in the thermal conductivity was offset by increasing specific heat. Consequently, thermal diffusivity exhibited continuous change with temperature in both the amorphous solid and supercooled liquid states as shown in Fig. 1.

Near room temperature, both phonons and electrons contribute to the thermal conductivity. The total conductivity, κ , is the sum of the two contributions, or

$$\kappa = \kappa_{\text{electron}} + \kappa_{\text{phonon}}, \quad (8)$$

where κ_{electron} and κ_{phonon} represent the electron and phonon thermal conductivities, respectively. The electron contribution to the thermal conductivity at temperature T can be estimated by the Wiedemann–Franz law

$$\kappa_{\text{electron}} = LT/R, \quad (9)$$

where L is the Lorenz number ($2.45 \times 10^{-8} \text{ W}\Omega\text{K}^{-2}$) and R the electronic resistivity of the materials.³² The electronic thermal conductivity of the Zr₄₁Ti₁₄Cu₁₂Ni₁₀Be₂₃ BMG at 300 K was calculated from the electrical resistivity measured in this study. The ratio of phonon to overall thermal conductivity, $\kappa_{\text{phonon}}/\kappa$, is listed in Table I. The thermal conductivities of Pd-based BMGs at 300 K that were reported by Harms²⁷ are listed in Table I. The Zr₄₁Ti₁₄Cu₁₂Ni₁₀Be₂₃ BMG has a higher phonon component than the Pd-based BMGs. This result will contribute to the ongoing discussion of the relationship between thermal conductivity and cluster size of BMGs.

In conclusion, we have measured thermal diffusivity of the amorphous solid and supercooled liquid in a

Zr₄₁Ti₁₄Cu₁₂Ni₁₀Be₂₃ BMG and the crystalline counterpart solid. The thermal diffusivity and conductivity of the amorphous solid were weakly temperature dependent, with small positive temperature coefficients. Furthermore, the amorphous solid showed lower thermal diffusivity and conductivity than the crystalline counterpart alloy. The thermal diffusivity of the supercooled liquid was quite constant with temperature. At room temperature, the thermal conductivity of Zr₄₁Ti₁₄Cu₁₂Ni₁₀Be₂₃ BMG was lower than that of Pd-based BMGs.

- ¹Z. P. Lu and C. T. Liu, *Acta Mater.* **50**, 3501 (2002).
- ²N. Nishiyama and A. Inoue, *Mater. Trans., JIM* **38**, 464 (1997).
- ³A. Inoue, T. Nakamura, T. Sugita, T. Zhang, and T. Masumoto, *Mater. Trans., JIM* **34**, 351 (1993).
- ⁴A. Inoue, A. Kato, T. Zhang, S. G. Kim, and T. Masumoto, *Mater. Trans., JIM* **32**, 609 (1991).
- ⁵A. Inoue, W. Zhang, T. Zhang, and K. Kurosaka, *Acta Mater.* **29**, 2645 (2001).
- ⁶X. H. Lin and W. L. Johnson, *J. Appl. Phys.* **78**, 6514 (1995).
- ⁷T. Zhang, A. Inoue, and T. Masumoto, *Mater. Trans., JIM* **32**, 1005 (1991).
- ⁸A. Peker and W. L. Johnson, *Appl. Phys. Lett.* **63**, 2342 (1993).
- ⁹J. Schroers, R. Busch, S. Bossuyt, and W. L. Johnson, *Mater. Sci. Eng., A* **304–306**, 287 (2001).
- ¹⁰Y. Kawamura, Y. Ohno, and A. Chiba, *Mater. Sci. Forum* **386–388**, 553 (2002).
- ¹¹Y. Kawamura, T. Shoji, and Y. Ohno, *J. Non-Cryst. Solids* **317**, 152 (2003).
- ¹²A. J. Swiston, T. C. Hufnagel, and T. P. Weihs, *Scr. Mater.* **48**, 1575 (2003).
- ¹³Y. Kawamura and Y. Ohno, *Scr. Mater.* **45**, 279 (2001).
- ¹⁴T. Shoji, Y. Kawamura, and Y. Ohno, *Mater. Sci. Eng., A* (in press).
- ¹⁵T. Shoji, Y. Kawamura, and Y. Ohno, *Mater. Trans., JIM* **44**, 1809 (2003).
- ¹⁶Y. Kawamura and Y. Ohno, *Scr. Mater.* **45**, 127 (2001).
- ¹⁷Y. Kawamura and Y. Ohno, *Mater. Trans., JIM* **42**, 2476 (2001).
- ¹⁸Y. Kawamura, S. Kagao, and Y. Ohno, *Mater. Trans., JIM* **42**, 2649 (2001).
- ¹⁹S. Kagao, Y. Kawamura, and Y. Ohno, *Mater. Sci. Eng., A* (in press).
- ²⁰R. Busch, A. Masuhr, and W. L. Johnson, *Mater. Sci. Eng., A* **304–306**, 97 (2001).
- ²¹R. Busch, Y. J. Kim, and W. L. Johnson, *J. Appl. Phys.* **77**, 4039 (1995).
- ²²R. Busch, Y. J. Kim, W. L. Johnson, A. J. Rulison, W. K. Rhim, and D. Isheim, *Appl. Phys. Lett.* **66**, 3111 (1995).
- ²³R. Busch and W. L. Johnson, *Appl. Phys. Lett.* **72**, 2695 (1998).
- ²⁴T. A. Waniuk, R. Busch, A. Masuhr, and W. L. Johnson, *Acta Mater.* **46**, 5229 (1998).
- ²⁵A. Masuhr, T. A. Waniuk, R. Busch, and W. L. Johnson, *Phys. Rev. Lett.* **82**, 2290 (1999).
- ²⁶Y. Kawamura and A. Inoue, *Appl. Phys. Lett.* **77**, 1114 (2000).
- ²⁷U. Harms, T. D. Shen, and R. B. Schwarz, *Scr. Mater.* **47**, 411 (2002).
- ²⁸C. L. Choy, K. W. Tong, H. K. Wong, and W. P. Leung, *J. Appl. Phys.* **70**, 4919 (1991).
- ²⁹T. A. Waniuk, J. Schroers, and W. L. Johnson, *Appl. Phys. Lett.* **78**, 1213 (2001).
- ³⁰W. J. Parker, R. J. Jenkins, C. P. Butler, and G. L. Abbott, *J. Appl. Phys.* **32**, 1679 (1961).
- ³¹A. Cezairliyan, T. Baba, and R. Taylor, *Int. J. Thermophys.* **15**, 317 (1994).
- ³²I. Kishimoto, T. Baba, and A. Ono, *Therm. Conduct.* **24**, 265 (1999).